# Interaction between the *Escherichia coli* Regulatory Protein TyrR and DNA: A Fluorescence Footprinting Study†

Michael Bailey,‡ Per Hagmar,‡,§ David P. Millar,|| Barrie E. Davidson,‡ Glenn Tong,⊥ Jim Haralambidis,⊥ and William H. Sawyer*,‡

*Department of Biochemistry and Molecular Biology and the Howard Florey Institute of Experimental Physiology and Medicine, University of Melbourne, Parkville, Australia, 3052, and the Department of Molecular Biology, Scripps Research Institute, MB20, 10666 North Torrey Pines Road, La Jolla, California 92037*

*Received April 5, 1995; Revised Manuscript Received August 14, 1995*⊗

ABSTRACT: The *Escherichia coli* regulatory protein TyrR controls the expression of eight transcription units that encode proteins involved in the biosynthesis and transport of aromatic amino acids. It is a homodimer of 57 600 subunit molecular weight and has a binding site for ATP and weak ATPase activity. In the presence of ATP, TyrR binds tyrosine, which induces self-association of TyrR from a dimer to a hexamer. This report examines the interaction of TyrR with a 42 bp DNA oligonucleotide containing a centrally located binding site for TyrR (TyrR box). Replacement of a thymidine residue with an aminouridine residue at positions 7, 9, 13, 15, 19, 22, and 26 from one end of the 42mer enables labeling with fluorescein and successive placement of the label along the major groove of the DNA. The fluorescence footprinting of the oligonucleotide was followed using steady-state and time-resolved fluorescence methods. Binding of the TyrR dimer caused significant changes in the fluorescent properties of the labels attached to positions 13, 15, and 26, suggesting the involvement of these bases in the binding of the protein. Except for the position 15 conjugate, binding of the TyrR dimer caused little change in fluorescence intensity. Therefore, fluorescence anisotropy was used to follow the binding equilibium. The fluorescence of the position 15 conjugate increased 1.6-fold on binding TyrR, suggesting that the fluorophore was in close contact with the protein. For all conjugates, the addition of tyrosine at the end of the titration with TyrR increased the anisotropy markedly, suggesting that the hexameric form of TyrR could bind the oligonucleotide. Two rotational correlation times were found for the labeled conjugates: one reflecting the motion of the probe at its point of attachment to the DNA (220−290 ps), the other reflecting the global tumbling of the labeled oligonucleotide (14−21 ns). On binding TyrR, changes in the correlation times and their associated amplitudes and changes in the range of angular motion of the probe depended on the position of the label. Evidence is presented that the binding of the TyrR hexamer, but not the TyrR dimer, affects regions that flank the binding sequence. The results support the hypothesis that the binding of the TyrR hexamer is responsible for interaction between tandem TyrR boxes in the *tyrR* regulon.

The regulatory protein TyrR is responsible for transcriptional regulation of the biosynthesis and transport of aromatic amino acids in *Escherichia coli.* It regulates the expression of eight unlinked operons, *aroFtyrA, aroLM, tyrB, aroP, tyrR, aroG, mtr,* and *tyrP*, which comprise the *tyrR* regulon. TyrR represses the transcription of the first six operons, it both represses and activates the transcription of *tyrP*, and it activates the transcription of *mtr.* The activity of TyrR is modulated by the binding of ATP and the aromatic amino acids (Pittard, 1987; Argaet et al., 1994; Wilson et al., 1995). In most cases, repression is mediated by tyrosine and is ATP dependent, whereas activation can be mediated by phenylalanine or tyrosine but does not require ATP (Pittard & Davidson, 1991).

Binding sites for TyrR located in the regulatory regions of the TyrR regulon are referred to as TyrR boxes and have the palindromic consensus sequence TGTAAAN$_6$TTTACA. Boxes that share strong homology with the consensus sequence have been shown *in vitro* to bind TyrR in the absence of aromatic amino acids and are referred to as strong boxes (Pittard & Davidson, 1991; Baseggio et al., 1990). In contrast, weak boxes usually share less than 10 identical residues with the consensus sequence and only bind TyrR when both ATP and tyrosine are present and when a strong box is nearby (Pittard & Davidson, 1991; Sarsero & Pittard, 1991; Lawley & Pittard, 1994).

TyrR exists as a homodimer of 57.6 kDa subunits in solution in the absence of coeffectors (Argaet et al., 1994). In the presence of tyrosine and ATP or in the presence of phenylalanine and ATP, TyrR self-associates from a dimer to a hexamer (Wilson et al., 1994). It has been proposed that hexamerization is essential *in vivo* for tyrosine-mediated repression since the estimated levels of intracellular tyrosine and TyrR are appropriate to thermodynamically control the

† Supported by grants from the Australian Research Council (to W.H.S. and B.E.D.) and Grant No. GM44060 from the U.S. National Institutes of Health (to D.P.M.). The Florey Institute is supported by a block grant from the National Health and Medical Research Council of Australia. M.B. is the recipient of an Australian Postgraduate Research Award. P.H. is the recipient of a Swedish Natural Research Council Fellowship.

* Author to whom correspondence should be addressed.
‡ University of Melbourne.
§ Present address: Department of Physical Chemistry, Chalmers University of Technology, S-412 96 Gothenburg, Sweden.
|| Scripps Research Institute.
⊥ Howard Florey Institute of Experimental Physiology and Medicine.

⊗ Abstract published in *Advance ACS Abstracts,* November 1, 1995.

0006-2960/95/0434-15802$09.00/0 

dimer−hexamer equilibrium (Wilson et al., 1994; Kwok et al., 1995). All operators sensitive to tyrosine-mediated repression possess a strong box/weak box pair arranged in tandem. In the case of the *aroFtyrA* and *aroLM* genes, a third TyrR strong box is present approximately 30 base pairs upstream of a strong box/weak box pair. For a two-box system it is postulated that the TyrR dimer is bound permanently to the strong box. It is further postulated that on binding tyrosine, the TyrR undergoes a conformational change that favors self-association to a hexameric structure that possesses three sites for the binding of TyrR boxes and in particular allows binding to a weak TyrR box of a strong box/weak box pair. This model suggests a looping or distortion of the DNA so that a single hexamer can bind to multiple boxes (Wilson et al., 1994; Lawley et al., 1994) and explains the more effective repression that has been observed in the presence of tyrosine.

The structure of the TyrR−DNA complex is not known. TyrR possesses a putative helix−turn−helix motif near its C-terminus (residues 482−502; Yang et al., 1993), and thus bases that line the major groove of the DNA in the TyrR box will be involved in binding the recognition helix of the helix−turn−helix motif. The current investigation was initiated (i) to explore the structural features of the DNA that are required for the recognition and binding of TyrR and (ii) to determine whether the TyrR hexamer binds to the operator site. We adopted a "fluorescent footprinting" approach whereby a fluorescent probe is conjugated separately to seven positions within or next to the TyrR box. Conjugation occurs at an amino group which is linked via a three-carbon spacer to the C5 of a uridine residue substituted for a thymidine residue in the primary sequence. The fluorophore therefore projects into the major groove of the DNA helix and can be progressively moved along the groove to determine those positions that interfere with the interaction between DNA and TyrR and/or influence the fluorescent properties of the probe. We used a fluorophore of high quantum yield (fluorescein) to provide the sensitivity required to approach the $K_d$ of the DNA−protein interaction, and we used steady-state and time-resolved fluorescence methods to characterize the binding equilibria and the rotational dynamics of the probe.

## MATERIALS AND METHODS

*Materials.* Fluorescein 5-isothiocyanate was purchased from Molecular Probes, Oregon. ATP and ATPγS were from Boehringer (Mannheim, Germany). Nucleotide phosphoramidites were from Applied Biosystems Inc. (Foster City, CA). Tyrosine was from Merck (Darmstadt, Germany). TyrR was purified from a genetically engineered strain of *E. coli* that overexpresses the protein (Argaet et al., 1994). Unless otherwise stated, molar concentrations of TyrR are expressed on a dimer basis.

*Synthesis of Labeled Oligonucleotides.* Oligonucleotides were synthesized on an Applied Biosystems model 381A synthesizer using standard phosphoramidite chemistry. In separate syntheses, selected thymidine residues in the base sequence were replaced by an aminouridine base [5-(3-aminoprop-1-yn-1-yl)-2′-deoxyuridine] as described previously (Hagmar et al., 1995). An oligonucleotide labeled at the 5′-position was synthesized using the standard Aminolink chemistry of Applied Biosystems which provides a six-carbon alkyl spacer between the probe and the 5′-phosphate of the DNA. After detritylation, dried oligonucleotides were dissolved in 200 mM $Na_2CO_3$, pH 10.0, to a concentration of about 1 mM. A 100-fold molar excess of fluorescein isothiocyanate (FITC) was added, and the reaction proceeded for 18 h in the dark at room temperature. Excess FITC was removed by passage through a column of Sephadex G-25. Fluorescein-labeled oligonucleotides were purified by reverse-phase C-18 HPLC as described (Hagmar et al., 1995). The labeling ratio was determined spectrophotometrically using extinction coefficients of 440 000 $M^{-1}$ $cm^{-1}$ for the 42mer at 260 nm (Hagmar et al., 1995) and 72 000 $M^{-1}$ $cm^{-1}$ for fluorescein at 495 nm. No correction was made for a change in the extinction of fluorescein on conjugation. Preparations possessed 1.0 ± 0.1 fluorescein molecules per 42mer. Equimolar amounts of the labeled primary strand and the unlabeled complementary strand were mixed and incubated at 90 °C for 5 min and then cooled at 0.5 °C/min. The purity of the double-stranded form was monitored by native PAGE. The melting temperature of the 19- and 22-labeled duplex was 1−2 °C lower than that of the unlabeled form (Hagmar et al., 1995). All fluorescence experiments were carried out on DNA solutions in a buffer of 100 mM KCl, 25 mM $KH_2PO_4/K_2HPO_4$, 1 mM EDTA, 0.1 mM dithiothreitol, 0.02% $NaN_3$, pH 7.4. The buffer was supplemented with 10 mM $MgCl_2$ and 200 μM ATP or ATPγS when required. TyrR possesses very weak ATPase activity (Argyropoulos, 1989; Cui et al., 1993). Since ATP is required for the binding of tyrosine, ATPγS, a nonhydrolyzable ATP analogue, was routinely included in solutions when measurements exceeded several hours.

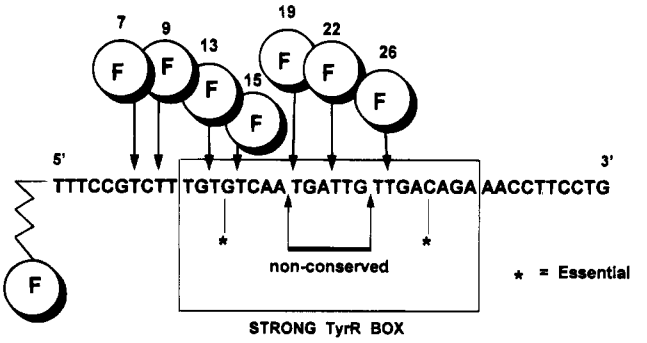


FIGURE 1: Design of oligonucleotides labeled at specific bases within, and to one side, of the TyrR strong box. The fluorescein label is denoted F, and the numbers refer to the position of the labeled residue from the 5′-terminus. In the labeled oligonucleotides, the thymidine residue at each labeling position is replaced by an aminouridine base [5-(3-aminoprop-1-yn-1-yl)-2′-deoxy-uridine]. The six nonconserved bases located centrally within the TyrR box are indicated together with the positions of essential C and G residues (*).

*Oligonucleotide Details and Nomenclature.* The single-stranded oligonucleotide shown in Figure 1 is referred to as 42A, and its complement is referred to as 42B. All labeling was on 42A. Labeled oligonucleotides are referred to as *x*F42A where the fluorescein (F) is at position *x* from the 5′-end of 42A. Thus a labeled double-stranded oligonucleotide is specified as *x*F42A/42B. Labeling was at positions (*x* =) 1, 7, 9, 13, 15, 19, 22, and 26. The labeled positions on the 42mer are shown in Figure 1, which also shows the centrally located variable six-base sequence within the TyrR box and the G and C bases at positions 14 and 29 which are known to be essential for binding of TyrR (Pittard &

Davidson, 1991; Lawley et al., 1994). The nucleotide sequence of 42A/42B corresponds to residues 218−259 of the *tyrR* operator (Cornish et al., 1986). Two other oligonucleotides, 22A/22B and 42NA/42NB, were also used. 22A/22B is a 22mer corresponding to the strong TyrR box in Figure 1; 42NA/42NB is a 42mer corresponding to residues 282−324 of the *tyrR* gene (Cornish et al., 1986).

*Steady-State Fluorescence Anisotropy.* Steady-state fluorescence measurements were made with a Perkin Elmer LS5 spectrofluorometer equipped with a thermostated cell block and a polarization accessory. Anisotropy measurements were made in the usual way, allowance being made for the grating correction factor (Lakowicz, 1983). Anisotropy titrations were made at 20 °C in 800 μL capacity microcells (path length 5 mm) or in 3.0 mL capacity standard cells (path length 10 mm). In a typical experiment, 5 μL aliquots of a TyrR stock solution (13 μM dimer) were added to 0.5 μM labeled DNA.

*Time-Resolved Fluorescence Measurements.* Time-resolved fluorescence intensity and anisotropy decays were acquired using the instrument described previously (Eis & Millar, 1993). Briefly, samples were repetitively excited at 514.5 nm using the output of a mode-locked argon laser (Coherent Innova 100, pulse duration 90 ps). The repetition rate of the laser pulses was reduced to 1.87 MHz using an external pulse selector. The samples were contained in a thermostated compartment at 20.0 °C. Fluorescence was collected 90° to the excitation beam, passed through a polarizer, dispersed by a monochromator, and detected by a microchannel plate photomultipler (Hamatasu R2809U-01) and a time-correlated single-photon counting system. Fluorescence emission was monitored at 530 nm with a bandpass of 4 nm. The emission polarizer was oriented 54.7° to the vertical excitation polarization for measurement of total fluorescence intensity decays or alternated between vertical and horizontal directions every 15 s under computer control for measurement of fluorescence anisotropy decays. Decay curves were collected in a multichannel analyzer until at least 10 000 single-photon counts had been accumulated in the peak channel. The decays were transferred to a Sparc 10 workstation for analysis. The instrument response function (110 ps full-width at half-maximum) was measured by scattering the laser pulses into the detector using a dilute suspension of nondairy coffee creamer.

The total intensity decay was analyzed using a discrete multiexponential model

$$I(t) = g(t) \otimes K(t) \tag{1}$$

$$\text{and} \quad K(t) = \sum_{i=1}^{N} \alpha_i \exp(-t/\tau_i) \tag{2}$$

where $I(t)$ is the fluorescence intensity at time $t$ after excitation, $K(t)$ describes the ideal decay of the fluorescence intensity, $g(t)$ is the instrument response function, ⊗ denotes convolution of two functions, $\alpha_i$ is the pre-exponential factor associated with each fluorescence lifetime $\tau_i$, and $N$ is the number of lifetime components. The lifetimes and preexponential factors were optimized for best fit using a nonlinear least-squares method (Bevington, 1969). The quality of the fit was judged by the value of the reduced chi-square parameter, $\chi_r^2$, and by examination of the weighted residuals.

When more than one lifetime was required to fit the decay of total fluorescence intensity, the average lifetime was expressed as

$$\tau = \sum_{i=1}^{N} \alpha_i \tau_i \tag{3}$$

Fluorescence decay curves measured with the emission polarizer either parallel, $I_{||}(t)$, or perpendicular, $I_{\perp}(t)$, to the vertical excitation polarization were analyzed according to eqs 4 and 5

$$I_{||}(t) = g(t) \otimes \{[1 + 2r(t)]K(t)\} \tag{4}$$

$$\text{and} \quad I_{\perp}(t) = g(t) \otimes \{[1 - r(t)]K(t)\} \tag{5}$$

where the time-dependent fluorescence anisotropy, $r(t)$, is represented by

$$r(t) = \sum_{k=1}^{2} r_{0k} \exp(-t/\phi_k) \tag{6}$$

and $K(t)$ is defined in eq 2. In eq 6, $r_{01}$ and $\phi_1$ are the amplitude and correlation time associated with local rotation of the probe, respectively, while $r_{02}$ and $\phi_2$ are the corresponding quantities describing overall rotation. The parameters $\phi_1$, $\phi_2$, $r_{01}$, and $r_{02}$ were freely optimized to obtain a simultaneous best fit of eqs 4 and 5 to $I_{||}(t)$ and $I_{\perp}(t)$ (Cross & Fleming, 1984). The lifetime parameters appearing in the expression for $K(t)$ were also optimized in this fit, and these converged to values that were essentially identical to those obtained from analysis of the total fluorescence intensity decay. The goodness of fit was judged as described above. The errors in the lifetimes and correlation times are the 95% confidence limits for these parameters.

The angular range of local dye rotation was estimated using a model of diffusion within a cone (Kinosita et al., 1977), with the cone semiangle given by

$$\theta = \cos^{-1}\{{}^1/_2[(1 + 8S)^{1/2} - 1]\} \tag{7}$$

where the order parameter, $S = [(r_0 - r_{01})/r_0]^{1/2}$, $r_0$ being the zero-time anisotropy and $r_{01}$ being the amplitude of the fast decay. The zero-time anisotropy was calculated by summing the fitted values of $r_{01}$ and $r_{02}$.

Steady-state anisotropies ($r_{ss}$) were calculated from time-resolved anisotropy data according to the relationship

$$r_{ss} = \frac{\int r(t)K(t)\,dt}{\int K(t)\,dt} \tag{8}$$

where $K(t)$ and $r(t)$ are given in eqs 2 and 6.

## RESULTS

*Preliminary Studies.* The strong box in the *tyrR* operator (Cornish et al., 1986) was used as the model for our analyses. This box (Figure 1) has a high degree of sequence symmetry and is identical to the TyrR box consensus sequence in 10 of its 22 residues. *In vitro* DNase footprinting studies with 300 bp DNA fragments have shown that this box binds TyrR strongly in the absence of tyrosine (P. Maroudas and B. E. Davidson, unpublished results). Gel retardation analysis was

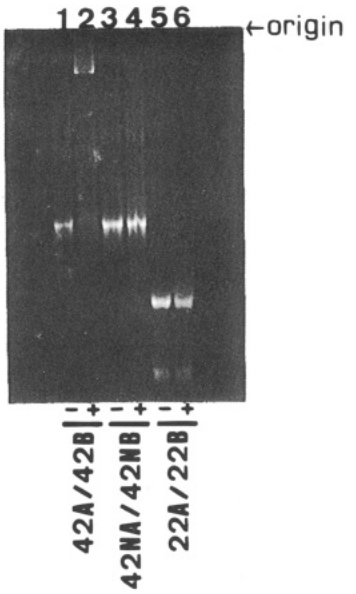


FIGURE 2: Nondenaturing PAGE of oligonucleotides in the presence (+) and absence (−) of TyrR. Lanes 1 and 2, 42A/42B; lanes 3 and 4, nonspecific 42mer, 42NA/42NB; lanes 5 and 6, 22A/22B. The ratio of TyrR dimer to oligonucleotide was 5:1. See Materials and Methods and Figure 1 for details of oligonucleotides.

used to determine the effect of oligonucleotide length on the binding of TyrR to this box. Figure 2 (lanes 5 and 6) shows that the 22 bp molecule (22A/22B) does not bind TyrR significantly under the conditions used. The presence of 10 bp flanking regions possessing the wild type *tyrR* operator sequence on each side of the TyrR box in the 42mer (42A/42B) significantly increased the binding affinity (Figure 2, lanes 1 and 2). Another 42mer (42NA/42NB), which has the nucleotide sequence of a region of the *tyrR* gene distant from the DNase TyrR footprint, failed to bind TyrR to any detectable extent (Figure 2, lanes 3 and 4). Analysis of the gel retardation patterns indicated a $K_d$ in the range 100−500 nM for the interaction of TyrR with 42A/42B (Hagmar et al., 1995). There was no change in the intrinsic tryptophan fluorescence of TyrR on binding 42A/42B, which was consistent with there being no tryptophan residues in the putative helix−turn−helix motif of the TyrR sequence.

*Fluorescence Titrations.* Except for 15F42A/42B, conjugates showed no change in fluorescein fluorescence intensity on binding TyrR. Fluorescence anisotropy was therefore used to monitor the binding equilibrium. The anisotropy titration of 7F42A/42B, which shows little (<10%) change in fluorescence intensity on binding TyrR, is shown in Figure 3. Addition of TyrR causes the anisotropy of the labeled oligonucleotide to increase from 0.112 to 0.126. No increase in anisotropy is observed for a similarly labeled nonspecific sequence (42NA/42NB) taken from a region downstream from a TyrR box. Nonlinear least-squares fitting of the data for 7F42A/42B, assuming the binding of one TyrR dimer per oligonucleotide, provides a $K_d$ of 0.20 $\mu$M. Addition of 305 $\mu$M tyrosine at the end of the titration caused the anisotropy to increase to 0.192, indicating a substantial increase in the size of the DNA−protein complex and/or an increase in the restriction of probe motion. The increase in anisotropy occurred within the time of the addition and measurement.

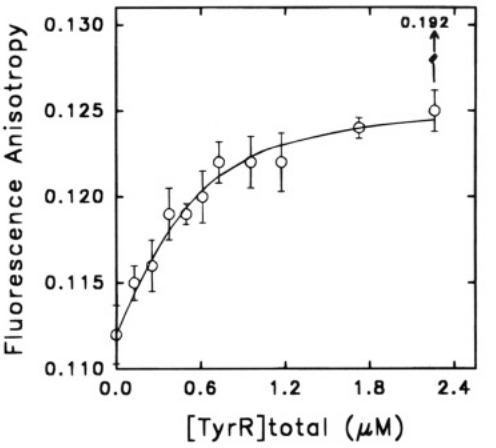


FIGURE 3: Steady-state fluorescence anisotropy titration of 7F42A/42B (0.5 $\mu$M) at 20 °C. The solid line is the nonlinear least-squares fit to the data ($K_d$ = 0.2 $\mu$M) assuming that one TyrR dimer binds to one oligonucleotide molecule. The broken arrow and figure indicate the increase in the anisotropy observed when tyrosine (305 $\mu$M) is added at the end of the titration. Excitation was at 495 nm and emission at 520 nm.

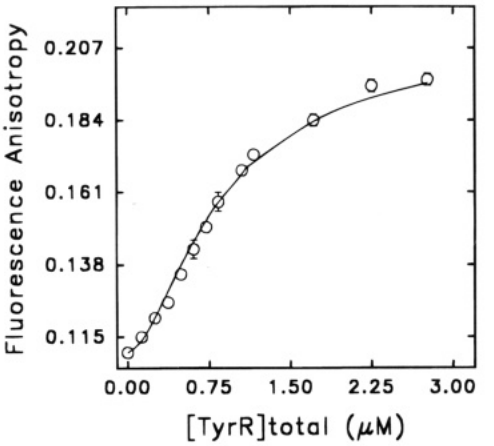


FIGURE 4: Steady-state fluorescence anisotropy titration of 7F42A/42B (0.5 $\mu$M) at 20 °C in the presence of 260 $\mu$M tyrosine. The solid line is for a model described in the Appendix which assumes a value of $2 \times 10^{11}$ $M^{-2}$ for the dimer−hexamer association constant, $2 \times 10^6$ $M^{-1}$ for the DNA−TyrR(dimer) association constant, and $7 \times 10^6$ $M^{-1}$ for the DNA−TyrR-(hexamer) association constant in all its forms (DNA:TyrR, 1:1, 2:1, and 3:1).

When the titration was carried out in the presence of 260 $\mu$M tyrosine, a large change in the anisotropy was observed and the resulting titration curve was sigmoidal as shown in Figure 4. The sigmoidality could have two possible origins. The tyrosine-induced self-association of TyrR from a dimer to a hexamer leads to a situation in which the ligand for the reaction (TyrR) exists as an equilibrium mixture of dimer and hexamer binding species. When a ligand self-associates and there is preferential binding of the higher molecular weight form to an acceptor, the resultant binding curve of fractional saturation versus total ligand concentration is sigmoidal (Nichol et al., 1969). Equivalent binding of the two forms leads to the more hyperbolic relationship. Alternatively, sigmoidality can be due to the greater increment in anisotropy which accompanies the binding of hexamer compared to the binding of dimer. At the beginning of the titration, TyrR concentrations are low, and on the basis of the association constant determined for TyrR in the absence of DNA (Wilson et al., 1994) most of the TyrR exists in the

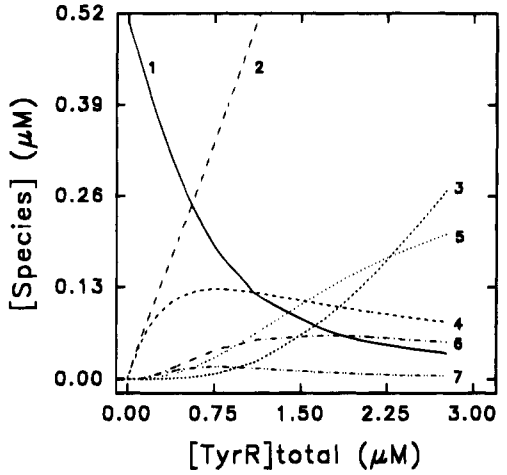


FIGURE 5: Calculated concentrations of species during the titration of the 42mer with TyrR. Free DNA (1), free $TyrR_{dimer}$ (2), free $TyrR_{hexamer}$ (3), DNA−$TyrR_{dimer}$ (4), (DNA)1−$TyrR_{hexamer}$ (5), (DNA)2−$TyrR_{hexamer}$ (6), and (DNA)3−$TyrR_{hexamer}$ (7). Assignment of anisotropies to the labeled species leads to the solid line shown in Figure 4 of the paper. The simulation was carried out as described in the Appendix. The values of the associations constants are listed in the caption to Figure 4.

dimeric form. Hence the increase in anisotropy on binding dimer is similar to that observed in Figure 3. As the TyrR concentration is increased during the titration, the formation of hexamer is favored. Assuming that the stoichiometry is preserved, that is, that the hexamer is able to bind three oligonucleotide molecules, there would be a greater increase in the hydrodynamic volume of the complex on binding the TyrR hexamer than on binding of the TyrR dimer and hence a greater increment in anisotropy.

To explore this latter possibility, the binding of a dimer−hexamer system to a single acceptor was simulated for given values of the association constants. We start by assuming a value for the dimer−hexamer association constant for TyrR in the absence of DNA but at saturating tyrosine concentrations similar to that reported previously (Wilson et al., 1994). We also assume initially that the association constant for the binding of hexamer to DNA was similar to that for the dimer ($7 \times 10^6$ $M^{-1}$), that is, that there is no preferential binding of dimer or hexamer species. The procedure for calculating the concentration of the individual species present during the course of the titration is described in the Appendix. These data are shown in Figure 5. We note the following characteristics: (1) the concentration of free DNA decreases as the titration proceeds (Figure 5, line 1); (2) a higher proportion of the free TyrR exists as dimer, its conversion to hexamer being favored as the titration proceeds (Figure 5, lines 2 and 3); (3) the concentration of the DNA−TyrR dimer complex reaches a maximum and then declines (Figure 5, line 4); (4) the concentrations of the $(DNA)_2$−$TyrR_{hex}$ and the $(DNA)_3$−$TyrR_{hex}$ complexes reach maxima early in the titration and then decline (Figure 5, lines 6 and 7). Therefore, the dominant DNA−hexamer TyrR complex present at the end of the titration is that with one of the three DNA-binding sites occupied by an oligonucleotide (Figure 5, line 5). Assuming realistic anisotropies for the oligonucleotide, the DNA−dimer complex and the DNA−hexamer complex, and noting the additivity of anisotropies according to the fractional concentrations of the species present it is possible to generate a simulated anisotropy titration curve. Such a

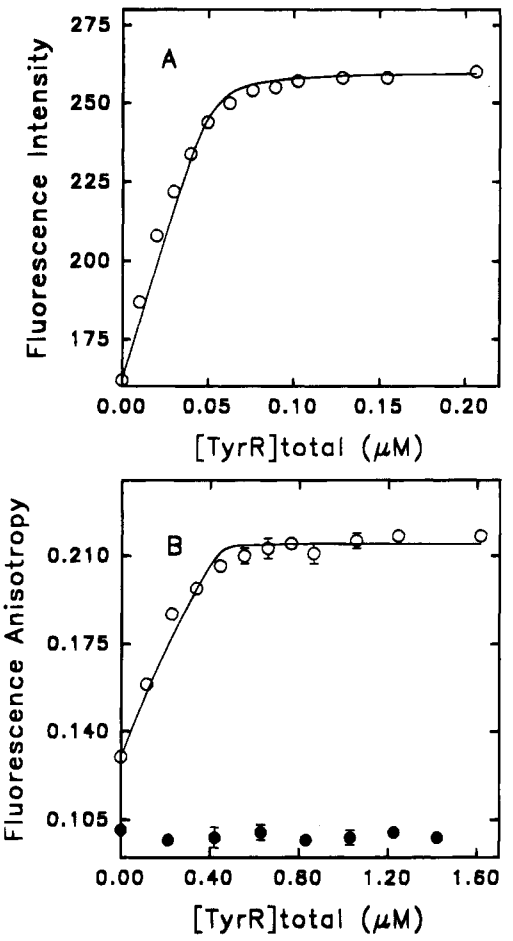


FIGURE 6: A, steady-state fluorescence intensity titration of 15F42A/42B (0.05 μM) at 20 °C. The solid line is the nonlinear least squares fit ($K_d$ = 1.1 nM) to the data. B, corresponding steady-state fluorescence anisotropy titration (open circles) of 15F42A/42B (0.46 μM) at 20 °C. The solid line is the fitted curve ($K_d$ = 1.0 nM) which takes into account the 30% enhancement of the fluorescence of the bound species. The titration of a labeled nonspecific sequence, 22F42NA/42NB (0.44 μM), is also shown (filled circles).

curve is shown in Figure 4 (solid line), the best fit to the experimental data being obtained assuming an association constant of $2 \times 10^6$ $M^{-1}$ for the for the binding of the dimer to DNA and $7 \times 10^6$ $M^{-1}$ for the binding of the hexamer to DNA, and a value of $2 \times 10^{11}$ $M^{-2}$ for the dimer−hexamer association constant. Simulations showed that the small difference in the binding affinities of the dimer and hexamer was not, by itself, sufficient to cause sigmoidality. We conclude that the sigmoidality of the titration can be adequately explained on the basis of the anisotropy increments which accompany the binding of the TyrR dimer and hexamer without invoking preferential binding of either the dimer or the hexamer to the DNA.

We now direct attention to the position 15 conjugate, 15F42A/42B, which showed a 1.6-fold enhancement in fluorescence on binding TyrR with only minor changes in the shape of the excitation and emission spectra. The quantum yield of fluorescein ($pK_a \approx 6.5$) is pH dependent, the protonated form being substantially quenched. The enhancement observed on binding TyrR suggests that the probe is located in a more basic environment created by the surface of the TyrR protein itself. The intensity titration is shown in Figure 6A. The binding is much tighter than that

Table 1: Fluorescence Lifetimes and Rotational Correlation Times Derived from Time-Resolved Fluorescence Experiments of the 5′-Labeled Oligonuceotide 1F42A and the Double-Stranded Species 1F42A/42B[a]

| | single strand | double strand |
|---|---|---|
| lifetimes (ns) | 1.29 ± 0.33 (0.14) | 1.51 ± 0.48 (0.11) |
| | 4.33 ± 0.06 (0.86) | 4.73 ± 0.07 (0.89) |
| correlation times (ns) | 0.40 ± 0.06 (0.250) | 0.29 ± 0.06 (0.200) |
| | 4.49 ± 0.94 (0.102) | 11.31 ± 1.15 (0.176) |

[a] Numbers in parentheses are the fractional decay amplitudes for the lifetimes and the decay amplitudes ($r_{01}$ and $r_{02}$, eq 6) for the correlation times.

observed for 7F42A/42B described above (Figure 3). The binding appears almost stoichiometric, the fitted curve providing an estimate of the upper limit of $K_d$ of 1.1 nM. The break-point in Figure 6A confirms the 1:1 stoichiometry assumed previously. The corresponding fluorescence anisotropy titration for this conjugate is shown in Figure 6B together with data for a nonspecific sequence labeled at the 22 position which shows no change in anisotropy on addition of TyrR. Note that much lower concentrations of labeled DNA can be accessed by intensity measurements than by anisotropy measurements due the decrease in the sensitivity of the instrument when polarizers are inserted in the optical path. The solid line in Figure 6B is the fitted curve ($K_d$ = 1 nM), but due to the intrinsic error in the anisotropy measurement (±0.002) $K_d$ values in the range $K_d$ = 0.5−5 nM adequately fitted the experimental data . The fitted curve takes into account the 30% enhancement of the fluorescence of the bound species. At the the higher concentrations of DNA used for titration of 7F42A/42B, calculation of intensity values from anisotropy measurements ($I = I_{\|} + 2I_{\perp}$) provided titration curves which were similar to the those obtained by direct measurement of intensity, indicating that the polarization anomalies were not significant in this system.

*Time-Resolved Fluorescence.* The fluorescence lifetimes and anisotropy decay parameters of the 5′-labeled single-stranded oligonucleotide 1F42A and the double-stranded species 1F42A/42B are summarized in Table 1. The decay of total fluorescence intensity for 1F42A can be fitted adequately to a function describing the sum of two exponentials with lifetimes of 1.29 and 4.33 ns and with 86% of the decay due to the longer-lifetime component. On forming the double-stranded species with the complementary strand, these lifetimes and their fractional amplitudes do not change appreciably ($\tau_1$ = 1.51 ± 0.48 ns, $\tau_2$ = 4.73 ± 0.07 ns). The anisotropy decay of 1F42A could be fitted to two correlation times ($\phi_1$ = 0.40 ± 0.06 ns, $\phi_2$ = 4.49 ± 0.94 ns). On formation of the double-stranded species, the shorter correlation time remained essentially unchanged ($\phi_1$ = 0.29 ± 0.06 ns) but the longer time increased to 11.31 ± 1.15 ns. We therefore attribute the shorter time to the motion of probe at its point of attachment and the longer correlation time to the global tumbling of the single- or double-stranded molecules. A characteristic anisotropy decay for 1F42A/42B is presented in Figure 7.

The lifetimes of probes located within the sequence were quenched ($\tau_{av}$ = 2.1−2.7 ns) relative to the probe at the 5′-terminal position ($\tau_{av}$ = 4.7 ns) but were independent of the position within the sequence. However, the decay of total fluorescence intensity was more complex at the internally labeled positions with three lifetimes being required to fit

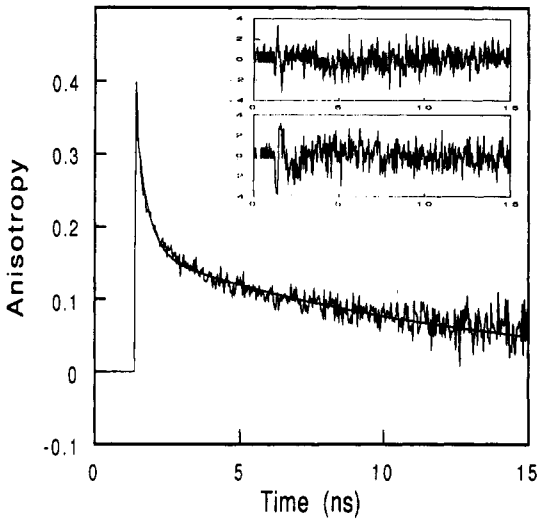


FIGURE 7: Time-resolved fluorescence anisotropy decay for the 5′-fluorescein-labeled oligonucleotide 1F42A/42B. The anisotropy was calculated from measured polarized intensity decays according to $r(t) = [I_{\|}(t) - I_{\perp}(t)]/[I_{\|}(t) + 2I_{\perp}(t)]$, where $r(t)$ is the time-dependent anisotropy, $I_{\|}(t)$ is the fluorescence intensity polarized parallel to the vertical excitation polarization, and $I_{\perp}(t)$ is the intensity of the perpendicular polarized fluorescence. The smooth anisotropy curve was calculated from the fitted intensity decays. The intensity decays were fitted to eqs 4 and 5, yielding correlation times of 409 ps and 11.9 ns ($\chi_r^2$ = 1.2). The insets show the weighted residuals from fitting the polarized intensity decays for the parallel (top inset) and vertical (bottom inset) components.

the data compared with two lifetimes for the probe at position 1. Anisotropy decays were adequately fitted by two correlation times which were independent of probe position ($\phi_1$ = 0.22−0.29 ns, $\phi_2$ = 14−21 ns). However, the amplitude associated with the fast correlation time was greater for the internally labeled duplexes ($r_{01}$ = 0.18−0.22) than for the 5′-labeled duplex ($r_{01}$ = 0.15). This may not necessarily indicate that the probe in the 5′-teminal position has a more restricted range of angular motion since the amplitude of the anisotropy decay is determined by the angle between the emission dipole and the axis of probe rotation as well as by the range of angular motion.

Total intensity and anisotropy decays were also obtained for mixtures of labeled oligonucleotides with the TyrR dimer and hexamer under saturating conditions of ATPγS (200 μM). Representative anisotropy decays for dimer and hexamer complexes with 7F42A/42B are shown in Figure 8A,B respectively together with the double-exponential fits of the experimental data. At the concentrations of DNA and TyrR used (0.45 μM oligonucleotide with a 5.3-fold molar excess of TyrR), more than 90% of the DNA is complexed with TyrR protein. Saturating tyrosine levels (200 μM) were used to promote polymerization to the hexamer. Under these conditions more than 90% of the DNA is complexed with TyrR protein. Global analysis of equilibrium distributions obtained with the analytical ultracentrifuge at multiple wavelengths (Bailey et al., manuscript in preparation) has also shown that under the conditions of our time-resolved anisotropy experiments more than 90% of the DNA is compexed with TyrR protein. We make the following points:

1. The average fluorescence lifetime for the dimer−DNA complex remains low for conjugates labeled at positions 1, 7, 9, 19, and 26 (2.1−2.7 ns). For the position 15 conjugate the average lifetime increases to 3.1 ns (Figure 9A). The average lifetimes for the hexamer−DNA complexes ($\tau_{av}$ =

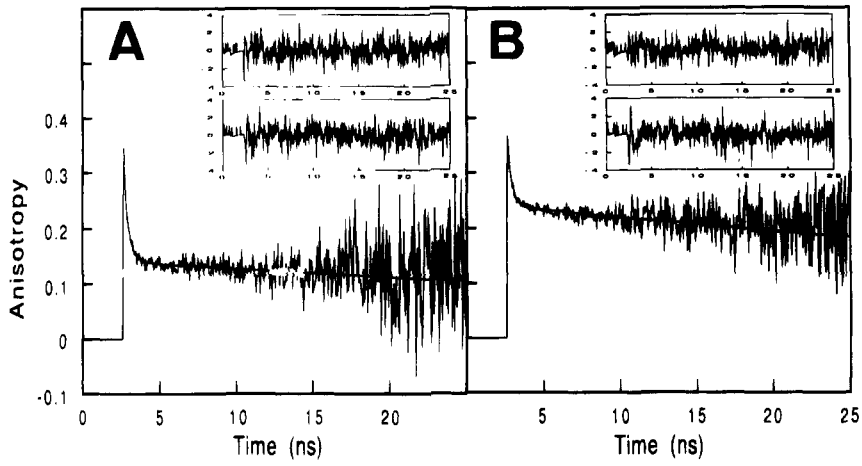


FIGURE 8: Time-resolved fluorescence anisotropy decay of internally labeled DNA bound to TyrR dimer or hexamer. A, anisotropy decay of 7F42A/42B duplex (0.5 $\mu$M) in the presence of 2.4 $\mu$M TyrR dimer. The experimental anisotropy curve was calculated from measured polarized intensity decays as explained in the caption to Figure 7. The smooth anisotropy curve was calculated from the fitted intensity decays. The best fit to the intensity decays yields correlation times of 207 $\pm$ 41 ps and 68.7 $\pm$ 39.4 ns ($\chi_r^2$ = 1.06). The weighted residuals from fitting the polarized intensity decays are shown in the inset with the parallel residuals in the top inset. B, as for A but in the presence of 475 $\mu$M tyrosine. The fitted anisotropy curve corresponds to correlation times of 162 $\pm$ 47 ps and 75.1 $\pm$ 23 ns ($\chi_r^2$ = 1.00).

2.4−3.1 ns) are higher than for the dimer−DNA complexes ($\tau_{av}$ = 2.1−2.6 ns) for conjugates labeled at positions 7, 9, 13, 19, 23, and 26. The average lifetime at position 15 is similar for the dimer−DNA and hexamer−DNA complexes ($\tau_{av}$ = 3.2 ns). A convenient way to express these relationships is to plot the percent increase in the average lifetime of the samples relative to the average lifetime of the free labeled oligonucleotide (Figure 9A) whereupon the effects of probe position and the binding of dimer and hexamer are readily discerned.

2. The anisotropy amplitude associated with the short correlation time was unaffected by the binding of the TyrR dimer except at positions 13 and 15 (and to a lesser extent at position 26) which showed a decreased amplitude. The data are plotted in Figure 9B in terms of the change in the amplitudes relative to that of the free double-stranded species. The binding of the hexamer caused a decrease in the amplitude of the fast correlation time at all probe positions including position 1. The anisotropy amplitude of the long correlation time changed in a complementary fashion such that the sum of the two amplitudes was constant and represented the limiting anisotropy of the probe (0.35−0.38). The half-cone angle for the motion of the dye at its point of attachment was determined from the amplitude of the faster component of the anisotropy decay according to eq 7. The half-cone angles and order parameters are summarized in Table 2. The half-cone angle was constant for the set of internally labeled oligonucleotides (41° $\pm$ 1°). On binding dimer, the half-cone angle decreased substantially at the 13, 15, and 26 positions but remained largely unchanged at other positions. However, the binding of the hexamer decreased the half-cone angle at all internal positions. The half-cone angles therefore mirror the trends noted above for the changes in the amplitude of the faster component of the anisotropy decay. The half-cone angle for the probe attached to the 5′-position was unaffected by the binding of the TyrR dimer and the TyrR hexamer and was relatively low (28−30°).

3. The observation that the amplitudes of the anisotropy decay are particularly sensitive to the binding of the TyrR hexamer suggests that a binding titration could be conducted using the amplitude parameters. Such an experiment is shown in Figure 10 where 7F42A/42B is added to a constant amount of TyrR in the presence of 500 $\mu$M tyrosine and 200 $\mu$M ATP$\gamma$S. The increase in the amplitude of the shorter correlation time and the corresponding decrease in that of the longer correlation time is clearly evident. In this experiment, the proportions of dimer and hexamer complex change as the titration proceeds and the resulting amplitudes have contributions from both species as well as from the uncomplexed DNA. It is therefore not appropriate to fit this data to obtain a binding constant.

4. A comparison of the time-resolved and steady-state measurements can be made by application of eq 8. For 7F42A/42B, the steady-state anisotropy (0.10−0.11) compares well with that derived from time-resolved measurements (0.128). On binding the TyrR dimer, the steady-state anisotropy increased by approximately 0.015 units; the increment calculated from the time-resolved anisotropy decays is 0.028. For 15F42A/42B, the steady-state anisotropy was 0.131 (compared to 0.148 derived from the time-resolved decay). On binding the dimer the values were 0.22 and 0.23, respectively. The agreement is reasonable given the differences in light source and slit widths of the two instruments. An increase in steady-state anisotropy can be due to an increase in the short or long correlation time or to a restriction in the angular motion of the probe at its point of attachment to the DNA, the latter being due to close contact between the probe and the binding protein. Except for the 13- and 15-position conjugates the binding of the TyrR dimer and hexamer marginally decreases the short correlation time (Table 2). At the 13- and 15-positions the short correlation time is almost unchanged but there is significant restriction in the angular motion of the probe (Table 2). At all positions, the binding of the TyrR dimer and hexamer increases the long correlation time and its associated amplitude (Table 3). We therefore conclude that for the 13-, 15-, and 26-position conjugates, the increase in the steady-state anisotropy on binding the TyrR dimer or hexamer is due to a decrease in the angular motion of the probe at its point of attachment to the DNA as well as to a decrease in the global tumbling of the complexes. For conjugates labeled at the other positions the smaller increase

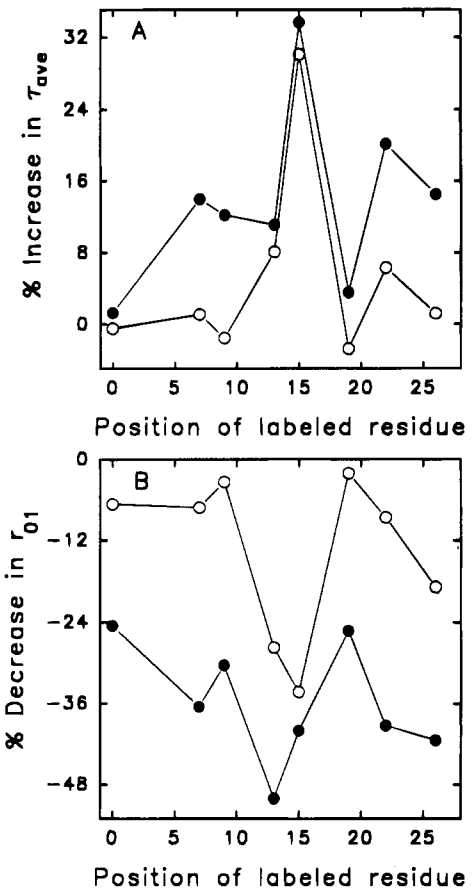


FIGURE 9: A, effect of the labeling position (from the 5′-terminus) on the change in the average lifetime of the labeled DNA in the presence of 2.4 $\mu$M TyrR dimer (open symbols) or 2.4 $\mu$M TyrR plus 470 $\mu$M tyrosine (filled symbols). The average lifetimes were calculated according to eq 3 and differences were determined relative to the value for the labeled oligonucleotide in the absence of TyrR and tyrosine. The error in the points is ±2.0 in terms of the ordinate scale. B, change in the amplitude of the shorter correlation time ($r_{01}$) as a function of the labeling position within the oligonucleotide sequence. Values are relative to the value for the labeled oligonucleotide in the absence of TyrR and tyrosine. The error in the points is ±5.0 in terms of the ordinate scale. Open and hollow symbols are as for A above.

Table 2: Half-Cone Angles ($\theta$, in deg) and Order Parameters ($S^2$) for Labeled Duplexes in the Presence and Absence of Dimeric and Hexameric TyrR[a]

| label position | DNA | | DNA-TyrR dimer | | DNA-TyrR hexamer | |
|---|---|---|---|---|---|---|
| | $\theta$ | $S^2$ | $\theta$ | $S^2$ | $\theta$ | $S^2$ |
| 1 | 35 | 0.55 | 34 | 0.57 | 27 | 0.72 |
| 7 | 46 | 0.35 | 41 | 0.44 | 31 | 0.63 |
| 9 | 46 | 0.35 | 44 | 0.39 | 33 | 0.59 |
| 13 | 41 | 0.44 | 31 | 0.63 | 25 | 0.75 |
| 15 | 39 | 0.47 | 29 | 0.67 | 27 | 0.72 |
| 19 | 41 | 0.44 | 41 | 0.44 | 32 | 0.62 |
| 22 | 44 | 0.38 | 41 | 0.45 | 29 | 0.67 |
| 26 | 41 | 0.44 | 34 | 0.57 | 27 | 0.72 |

[a] $\theta$ values are presented ±1; $S^2$ values are presented ±0.25.

in steady-state anisotropy on binding dimer is due largely to the decrease in the global tumbling of the complexes, and not to a restriction of the local motion of the probe, suggesting that the probe is not in close contact with the protein. We would therefore predict that the increment in steady-state anisotropy on binding the TyrR dimer would

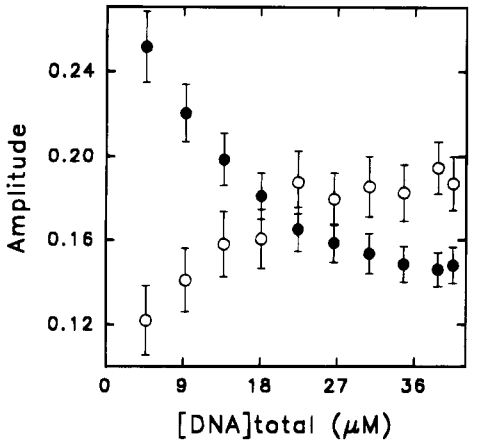


FIGURE 10: Changes in the amplitudes associated with the short ($r_{01}$, open symbols) and long ($r_{02}$, filled symbols) correlation times derived from the anisotopy decay of 7F42A/42B on the addition of the labeled oligonucleotide to TyrR (30 $\mu$M) in the presence of 500 $\mu$M tyrosine and 200 $\mu$M ATP$\gamma$S.

be greater for the 15-position conjugate than for the 7-position conjugate. This is indeed the case as can be seen from a comparison of the titration data in Figures 3 and 6B. The time-resolved data also provide an explanation for why the TyrR hexamer causes a larger increase in steady-state anisotropy upon binding to any of the labeled conjugates than does binding of the TyrR dimer. Hexamer binding causes significant restriction of probe motion at all labeled positions (Table 2) and also results in slower global tumbling (Table 3). However, we would point out the large errors associated with the determination of $\phi_2$ because of the relatively short lifetime of the fluorophore.

## DISCUSSION

DNAse footprinting provides little information about nucleotides which are intimately involved in the association between DNA and protein.The resolution provided by hydroxyl radical footprinting is greater (Dixon et al., 1991). The fluorescence footprinting approach described previously (Guest et al., 1991; Carver et al., 1994) and adopted in the current investigation can reveal subtle variations in the local environment of specific labeled bases within the protein binding site. Amino acid residues at the DNA binding surface of the protein that are located close to the probe can restrict the local motion of the probe, the degree of restriction being evident in the fluorescence anisotropy, and in certain cases causes alterations in the fluorescence lifetime (Guest et al., 1991). Furthermore, the fluorescence footprinting approach may be used to measure the thermodynamics of the interaction and to analyse complex binding interactions involving proteins that bind DNA with more than one footprint (Carver et al., 1994). The approach also has the advantage that resonance energy transfer strategies can be adopted to acquire structural information on the DNA−protein complex, a particular advantage in the case of high molecular weight complexes which might not be amenable to X-ray crystallographic investigation. The choice of fluorescein as a probe was dictated by the requirement for a high quantum yield so that, given the sensitivity of the instrument detection systems available, DNA concentrations approaching the dissociation constant of the DNA−protein interaction could be accessed.

Table 3: Correlation Times ($\phi_1$ and $\phi_2$) Associated with the Time-Resolved Anisotropy Decays of *x*F42A/42B Conjugates and Their Complexes with the TyrR Dimer and Hexamer

| probe position | $\phi_1$ (ps) | | | $\phi_2$ (ns) | | |
|---|---|---|---|---|---|---|
| | DNA alone | DNA−dimer complex | DNA−hexamer complex | DNA alone | DNA−dimer complex | DNA-hexamer complex |
| 1 | 408 ± 68 | 500 ± 82 | 77 ± 36 | 12 ± 1 | 28 ± 3 | 73 ± 9 |
| 7 | 262 ± 40 | 207 ± 41 | 162 ± 47 | 18 ± 5 | 69 ± 39 | 75 ± 23 |
| 9 | 279 ± 47 | 230 ± 43 | 256 ± 61 | 15 ± 4 | 41 ± 15 | 138 ± 86 |
| 13 | 283 ± 59 | 370 ± 107 | 392 ± 149 | 14 ± 3 | 25 ± 4 | 65 ± 18 |
| 15 | 293 ± 65 | 414 ± 100 | 309 ± 92 | 16 ± 3 | 38 ± 6 | 79 ± 20 |
| 19 | 230 ± 43 | 225 ± 41 | 172 ± 49 | 18 ± 3 | 51 ± 17 | 99 ± 36 |
| 22 | 221 ± 36 | 207 ± 40 | 171 ± 49 | 21 ± 5 | 98 ± 58 | 94 ± 27 |
| 26 | 277 ± 59 | 315 ± 80 | 237 ± 82 | 15 ± 3 | 23 ± 4 | 65 ± 15 |

The substitution of an aminoalkynyluridine for a thymidine provides a convenient way of labeling the DNA without interfering with the base pairing. When the amino group is attached through C5 of uridine and subsequently conjugated to fluorescein, the fluorophore resides in the major groove of the DNA and may or may not interfere with those amino acid residues of a protein that occupy the major groove of the DNA. In the current investigation the effects of dimer binding were most obvious in oligonucleotides labeled at positions 13, 15, and, to a lesser extent, 26, as reflected by the increase in the average lifetime, and the decrease in the amplitude of the short correlation time which can be interpreted as a decrease in the half-cone angle for the motion of the probe at its point of attachment (Figure 9, Table 2). Residues 13, 15, and 26 are close to the highly conserved G and C residues at positions 14 and 29, respectively. Substitution or deletion of these residues reduces or abolishes repression or activation of transcription, and abolishes protection to DNase of both strong and weak boxes (Pittard & Davidson, 1991), suggesting that TyrR is in intimate contact with these bases. The observed perturbations of the properties of the fluorophore at positions 13, 15, and 26 are therefore consistent with these observations. Interestingly, labeling within the central nonconserved 6 bp segment of the TyrR box is relatively insensitive to the binding of dimer, implying that the dimer does not make close contacts in this region. Similarly, positions directly adjacent to the TyrR box (7 and 9) are relatively insensitive to the formation of the dimer−DNA complex. The evidence therefore points to bases 13−14 and 26−29 as playing an important role in the interaction with the dimeric repressor protein.

Labeling at position 15 appears to be unique in that it is the only position where the intensity of the fluorophore is appreciably enhanced by the binding of the repressor. Fluorescein fluorescence is not very sensitive to the polarity of its local environment. However, changes in pH induce changes in both the extinction coefficient and the quantum yield (Rozwadowski, 1961). The enhancement may reflect a more basic environment or an induced change in the $pK_a$ of the probe caused by the proximity of the probe to the surface of the repressor protein itself. Alternatively, the enhancement may be due to a relief of internal quenching. Millar et al. (1992) suggested that the quenching of fluorescein conjugated to DNA may be due to hydrogen bonding between the hydroxyl group of the xanthine ring of fluorescein and the exocyclic amino group of a 5′-cytosine. The quantum yield of free fluorescein is quenched by hydrogen bonding between the hydroxylate anion and protic solvents. The cytosine at position 14 may serve this purpose and its interaction with fluorescein may be relieved on formation of the TyrR−DNA complex.

The higher affinity noted for the position-15 conjugate also suggests that the fluorophore contributes to the binding energy of the interaction. The carboxylate group of fluorescein would be about 90% ionised at pH 7.4. Helix 1 of the putative helix−turn−helix DNA binding motif of TyrR comprises nine amino acid residues, including two arginines and two lysines. The negative charge of fluorescein may interact with one or more of these basic residues in TyrR, and contribute positively to the binding energy. We have observed a similar effect on the binding energy when coumarin is conjugated to position 22 of the oligonucleotide (M. Bailey and W. H. Sawyer, unpublished data). Thus, fluorescent labeling of a protein binding site on DNA may enhance or hinder the binding process.

A close association of the fluorescein in the 15 position with the repressor protein is also suggested by the time-resolved data. The average lifetime of the fluorescein is increased by about 30% on binding the TyrR dimer or hexamer (Figure 9A). Moreover, the motion of the probe at its point of attachment becomes slower as evident by the apparent increase in the value of $\phi_1$. Concomitantly, the range of fluorophore's angular motion decreases substantially as indicated by the smaller amplitude associated with $\phi_1$ (Figure 9B).

Of particular interest are the changes that occur within the 10 bp flanking region at positions 7 and 9 of the oligonucleotides, and also at positions 19 and 22 within the nonconserved 6 bp central element. In these regions, the binding of the TyrR dimer does not affect the average lifetime of the probe nor its range of angular motion (Figure 9A,B). In contrast, the binding of the hexamer increases the average lifetime and restricts the angular motion. These sites are therefore in closer contact with the repressor protein when that protein exists as a hexamer than when it exists as a dimer. This suggests that the hexamer either provides extra surface with which the flanking and internal regions can make contact with the protein surface, or distorts the DNA so that spatially distant regions are brought into contact with the protein surface. Circular dichroism of the DNA−TyrR complex may be a useful way of approaching the latter possibility.

The finding of substantial changes in the steady-state and time-resolved anisotropy of the DNA in the presence of the TyrR hexamer is the first evidence that DNA can occupy one or more sites on the hexamer. The values obtained for the DNA−dimer and DNA−hexamer association constants were so similar as to suggest equivalent binding of the 42mer

to each form. The value obtained for the hexamerisation constant ($K_{DH} = 2 \times 10^{11}$ $M^{-2}$) was approximately one order of magnitude lower than that reported by Wilson et al. (1994) for TyrR in the absence of DNA. That three sites may be occupied by the hexamer has physiological significance since weak TyrR boxes are only occupied in the presence of tyrosine (Pittard & Davidson, 1991; Andrews et al., 1991a,b), suggesting that the DNA may loop back to occupy a vacant site on the hexamer. The finding that tyrosine could induce the dimer−hexamer association of TyrR gave new impetus to this proposal (Wilson et al., 1994). In the *tyrP* and *aroFtyrA* systems, maximum repression is observed when the distance between strong and weak boxes is a multiple of the pitch of the DNA helix indicating that looping would require a particular face of the DNA to be presented to the binding site on the repressor (Andrews et al., 1991a). The rapidity with which the addition of tyrosine at the end of a titration of labeled DNA with TyrR increases the steady-state anisotropy suggests that the repressor may not dissociate from the operator site before self-associating to the hexamer as proposed by Wilson et al.(1994). That is, the self-association may occur while the TyrR is attached to the DNA. Such a mechanism would require the DNA binding site in the C-terminal domain of TyrR to be well separated from the interaction sites between dimer units in the hexamer.

## APPENDIX

Numerical Simulation of the Binding of a Self-Associating Ligand to a Monovalent Acceptor

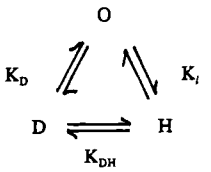


The self-association of the repressor protein from a dimer (D) to a hexamer (H) is described by an association constant ($K_{DH}$).

$$3D \rightleftharpoons H \qquad [H] = K_{DH}[D]^3$$

The binding of a single 42mer oligonucleotide (O) to a dimeric repressor is described by an association constant $K_D$. Successive binding of the oligonucleotide to three sites on the hexameric form of repressor have association constants $K_i = K_1$, $K_2$, and $K_3$. The concentration of the individual species is therefore given by

$$D + O \rightleftharpoons DO \qquad [DO] = K_D[O][D]$$

$$H + O \rightleftharpoons HO \qquad [HO] = K_{DH}K_1[D]^3[O]$$

$$HO + O \rightleftharpoons HO_2 \qquad [HO_2] = K_{HD}K_1K_2[D]^3[O]^2$$

$$HO_2 + O \rightleftharpoons HO_3 \qquad [HO_3] = K_{HD}K_1K_2K_3[D]^3[O]^3$$

Conservation of mass provides that the total concentration of O in all its forms ($[O]_T$) is given by

$$[O]_T = [O'] + [DO] + [HO] + 2[HO_2] + 3[HO_3] \quad (A1)$$

where [O] is a first estimate of [O] and [O′] (below) is a new estimate of [O].

$$[O'] = [O]_T - K_D[O][D] - K_{DH}K_1[D]^3[O] - 2K_{DH}K_1K_2[D]^3[O]^2 - 3K_{DH}K_1K_2K_3[D]^3[P]^3 \quad (A2)$$

Similarly, the total concentration of TyrR dimers $[D]_T$ is given by

$$[D]_T = [D'] + [DO] + 3[H] + 3[HO] + 3[HO_2] + 3[HO_3] \quad (A3)$$

where [D] is a first estimate of [D] and [D′] (below) is a new estimate of [D].

$$[D'] = [D]_T - K_D[O][D] - 3K_{DH}[D]^3 - 3K_{DH}K_1[D]^3[O] - 3K_{DH}K_1K_2[D]^3[O]^2 - 3K_{DH}K_1K_2K_3[D]^3[O]^3 \quad (A4)$$

Input parameters for the simulation are $K_{DH}$, $K_D$, $K_1$, $K_2$, $K_3$, $[O]_T$, and $[D]_T$. Initial estimates are made of [O] and [D]. [O′] is calculated from eq A2 and substituted for [O] in eq A4 to determine [D′]. The values of [O′] and [D′] are substituted into eq A2, and the process reiterated until there is no difference between [O] and [O′] nor between [D] and [D′]. The process is repeated for a new value of $[D]_T$ so that the concentration of the individual species can be plotted against the total concentration of repressor (Figure 6). For the purposes of the preceding paper it is assumed that there is no cooperativity between binding sites on the hexamer. Therefore, the intrinsic binding constants are identical and the macroscopic binding constants are related by a statistical factor $K_1:K_2:K_3 = 3:1:1/3$.

For comparison with experimental binding curves (anisotropy *versus* [TyrR]), the total anisotropy was determined by summing the fractional contributions of the individual species.

$$r = \sum f_i r_i = f_O r_O + f_{DO} r_{DO} + f_{HO} r_{HO} + f_{HO2} r_{HO2} + f_{HO3} r_{HO3} \quad (A5)$$

where $f_i$ are the fractional concentrations of the $i$th fluorescing species whose anisotropies ($r_i$) were estimated from experiment ($r_O = 0.110$, $r_{DO} = 0.130$, $r_{HO} = r_{HO2} = r_{HO3} = 0.222$).

## ACKNOWLEDGMENT

We thank Ted Carver for assistance with the time-resolved fluorescence measurements, Peter Maroudas for assistance with the preparation of TyrR, and Tim Wilson for helpful discussion of the manuscript.

## REFERENCES

Argyropoulas, V. P. (1989) Ph. D. Thesis, University of Melbourne, Victoria, Australia.
Andrews, A. E., Dickson, B., Lawley, B., Cobbett, C., & Pittard, A. J. (1991a) *J. Bacteriol. 173*, 5079−5085.
Andrews, A. E., Lawley, B., & Pittard, A. J. (1991b) *J. Bacteriol. 173*, 5068−5078.
Argaet, V. P., Wilson, T. J., & Davidson, B. E. (1994) *J. Biol. Chem. 269*, 5171−5178.
Bassegio, N., Davies, W. D., & Davidson, B. E. (1990) *J. Bacteriol. 172*, 2547−2557.

Bevington, P. R. (1969) *Data Reduction and Error Analysis for the Physical Sciences,* McGraw-Hill, New York.
Carver, T. E., Hochstrasser, R. A., & Millar, D. P. (1994) *Proc. Natl. Acad. Sci. U.S.A. 91*, 10670−10674.
Cornish, E. C., Argyropoulas, V. P., Pittard, A. J., & Davidson, B. E. (1986) *J. Biol. Chem. 261*, 403−412.
Cross, A. J., & Fleming, G. R. (1984) *Biophys. J. 46*, 45−56.
Cui, J., Ni, L., & Somerville, R. L. (1993) *J. Biol. Chem. 268*, 13023−13025.
Dixon, W. J., Hayes, J. J., Levin, J. R., Weidner, M. F., Dombroski, B. A., & Tullius, T. D. (1991) *Methods Enzymol. 208*, 380−413.
Eis, P. S., & Millar, D. P. (1993) *Biochemistry 32*, 13852−13860.
Guest, C. R., Hochstrasser, R. A., Dupuy, C. G., Allen, D. J., Benkovik, S. J., & Millar, D. P. (1991) *Biochemistry 30*, 8759−8770.
Hagmar, P., Bailey, M., Tong, G., Haralambidis, J., Sawyer, W. H., & Davidson, B. E. (1995) *Biochim. Biophys. Acta 1244*, 259−268.
Kinosita, K., Kawato, S., & Ikegami, A. (1977) *Biophys. J. 20*, 289−305.
Kwok, T., Yang, J., Pittard, A. J., Wilson, T. J., & Davidson, B. E. (1995) *Mol. Microbiol. 17*, 471−481.
Lakowicz, J. R. (1983) *Principles of Fluorescence Spectroscopy*, Plenum Press, New York.
Lawley, B., & Pittard, A. J. (1994) *J. Bacteriol. 176*, 6921−6930.
Millar, D. P., Hochstrasser, R. A., Guest, C. R., & Chen, S.-M. (1992) in *Time-Resolved Laser Spectroscopy in Biochemistry III,* SPIE Proceedings Series 1640, pp 592−598.
Nichol, L. W., Smith, G. D., & Ogston, A. G. (1969) *Biochim. Biophys. Acta 184*, 1−10.
Pittard, A. J. (1987) in *Escherichia coli and Salmonella typhimurium: Cellular and Molecular Biology* (Neidhardt, F. C., Ingraham, J. L., Brooks-Low, K., Magasanik, B., Schaechter, M., & Umbarger, H. E., Eds.), pp 368−394, American Society for Microbiology, Washington, DC.
Pittard, A. J., & Davidson, B. E. (1991) *Molec. Microbiol. 5*, 1585−1592.
Rozwadowski, M. (1961) *Acta Phys. Pol. 20*, 1005−1017.
Sarsero, J. P., & Pittard, A. J. (1991) *J. Bacteriol. 173*, 7701−7704.
Wilson, T. J., Argeat, V. P., Howlett, G. J., & Davidson, B. E. (1995) *Mol. Microbiol. 17*, 483−492.
Wilson, T. J., Maroudas, P., Howlett, G. J., & Davidson, B. E. (1994) *J. Mol. Biol. 238*, 309−318.
Yang, J., Ganesan, S., Sarsero, J., & Pittard, A. J. (1993) *J. Bacteriol. 175*, 1767−1776.

BI9507645